

## Evaluation of energy release rate of composites laminated with finite element method

Habib Achache<sup>\*1</sup>, Benali Boutabout<sup>1</sup>, Abdelouahab Benzerdjeb<sup>3</sup> and Djamel Ouinas<sup>2</sup>

<sup>1</sup>Laboratory of Mechanical and Physical of Materials (LMPM), University Djillali Liabes of Sidi Bel Abbes, BP 89, Street Ben M'Hidi, Sidi Bel Abbes, Algeria

<sup>2</sup>Laboratory of Numerical and experimental modeling of mechanical phenomena, University of Mostaganem, Route Belahcel 27000 Mostaganem, Algeria

<sup>3</sup>University of Science and Technology Oran Mohammed Boudiaf (USTO), BP1505 El Menaouar, 31036 Oran, Algeria

(Received August 4, 2014, Revised December 24, 2014, Accepted June 9, 2015)

**Abstract.** Control of the mechanical behavior of composite materials and structures under monotonic and dynamic loads for cracks and damage is a vast and complex area of research. The modeling of the different physical phenomena and behavior characteristics of a composite material during deformation play an important role in the structural design. Our study aims to analyze numerically the energy release rate parameter  $G$  of a composite laminated plate (glass or boron / epoxy) cross-ply  $[+\alpha, -\alpha]$  in the presence of a crack between two circular notches under the effect of several parameters such as fiber orientation  $\alpha$ , the crack orientation  $\beta$ , the orientation  $\gamma$  of the two considered circular notches and the effect of mechanical properties. Our results show clearly that both notches orientation has more effect on  $G$  than the cracks and fibers orientations.

**Keywords:** cracks; rate of energy restitution; fibers orientations; finite element method and laminates

### 1. Introduction

Thermoset composites reinforced with different types of fibers are used in the transport sector, including aerospace and automotive. They are widely used in applications where weight reduction is critical. More, the use of a material is enlarged more probability of possible failure is increased. The ability to characterize ruptures, for example in terms of identifying failure modes, characteristic parameters or rupture critical values, is essential to ensure the integrity of parts and services for the design of future products. The main aspect of this failure is the crack, which provides the location and progression of the fracture. The study of an existing crack and its stability is of great importance. In reality, the propagation of a crack can lead to rupture of a component that may lead to the total collapse of the structure. The fracture mechanics is the right

---

\*Corresponding author, Ph.D. E-mail: [achachehabib@yahoo.fr](mailto:achachehabib@yahoo.fr)

<sup>a</sup>Professor, E-mail: [bboutabout@yahoo.fr](mailto:bboutabout@yahoo.fr)

<sup>b</sup>Professor, E-mail: [douinas@netcourrier.com](mailto:douinas@netcourrier.com)

tool to analyze this situation based on the fracture characteristics of the material that are the critical stress intensity factor ( $K_c$ ) and the critical energy release rate ( $G_c$ ) also called tenacity. This degradation of the composite was studied by many authors.

Experimentally, it has been observed that the different mechanisms of damage in the transverse cross-laminates are cracking, delamination crack tip and the longitudinal or interlaminar cracking. (Bai and Pollard 1999). The order and sequence of occurrence of such damage depends mainly on the following parameters: nature of the fiber constituents / matrix architecture of the laminated plate, and the manufacturing process of shaping and different types of loads. The final collapse of the composite is the result of the spread and accumulation of these three types of damages. In the literature, these damages have generally been studied separately: studies focus either on crack propagation by either an analytical or numerical method (Berthelot and Le Corre 2000) or an analytical model of delamination (Rebière *et al.* 2002). Haneef *et al.* (2011) have carried out finite element analysis to analyze the delamination effect on composite structures with two models. Smith B. W. determined the angle of crack propagation and found to be more with the mode I contribution 55% and decrease slightly above this value (Smith 1993). A survey was conducted again by TODO *et al.* using the model and mode II ENF (End Notched Flexure) composite glass-fibre/vinylester (Todo *et al.* 2000). It was concluded that in the loading of the crack growth, in mode II, is a function of fiber / matrix interface properties. However, some authors studied the role of transverse cracks in the initiation of delamination between layers based on properties. For example, Wang and Karihaloo (1997) study the best stack ( $0^\circ$ ,  $45^\circ$ ,  $90^\circ$ ) to reduce the stress concentration at the crack tip and the interface shear stress in mode II. (Dasa *et al.* 2013) studied the effect of cap and wrap-around on reducing the stress concentration at the crack which leads to suggest the propagation of cracks. TODO and JAR presented a finite element study micro-macro - mechanical growth of interlaminar crack array fiberglass / epoxy DCB specimens for mode I (Todo and Jar 1998). Due to the heterogeneity of the composite material, probabilistic studies have also been carried out by two approaches: some (Manders *et al.* 1983) use a probabilistic criterion for the distribution of critical stress while (Katerelos *et al.* 2008) use a criterion of the randomized critical energy release rate. Szekrényes (2012) has shown that the interface shear stress contributes significantly only to the mode-II energy release rate. Qing *et al.* (2011) have located a semi analytical model of energy release rate for delamination analysis of composites. Yao *et al.* (2014) have used the energy deformation refund rate for the characterization of fatigue delamination. Bouziane *et al.* (2014) have developed a numerical method by mixed finite element associated with the virtual crack extension technique to assess the energy release rate twisting of cracks.

Our study aims to analyze numerically by the finite element method the effect of the orientation of the crack, placed between two circular notches, on the energy release rate, taking into account several parameters such as the fiber orientation, the orientation of the two notches and the effect of mechanical properties.

## 2. Geometric model

Our model is an orthotropic square plate of  $100 \times 100 \text{ mm}^2$  consisting of eight crossed plies  $[+\alpha -\alpha]$  0.125 mm thick; each layer of an epoxy matrix is reinforced by glass or bore fibers Fig. 1. The material mechanical properties of the unidirectional composites are shown in Table 1 (Seo and Lee 2002). The laminate plaque presents two identical circular notches whose positions is defined by the interdistance (Achache *et al.* 2013), passing through the center of the plate and oriented at an

Table 1 Mechanical properties of composites

Proprieties	E11[MPa]	E22[MPa]	E33[MPa]	$\nu_{12}$	$\nu_{13}$	$\nu_{23}$	$G_{12}$ [MPa]	$G_{13}$ [MPa]	$G_{23}$ [MPa]
Glass/epoxy	50000	14500	14500	0.33	0.33	0.33	2560	2560	2240
Boron/epoxy	208000	25400	25400	0.1677	0.1677	0.035	7200	7200	4900

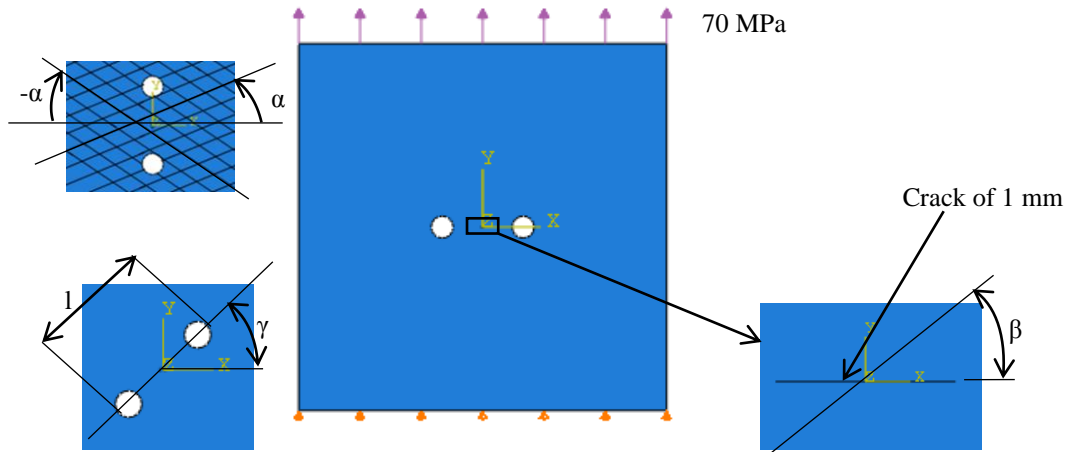


Fig. 1 Geometric model

- $l$ : distance between two circular notches
- $\alpha$ : angle of fiber orientation
- $\beta$ : angle of the crack orientation
- $\gamma$ : angle of the two circular notches orientation

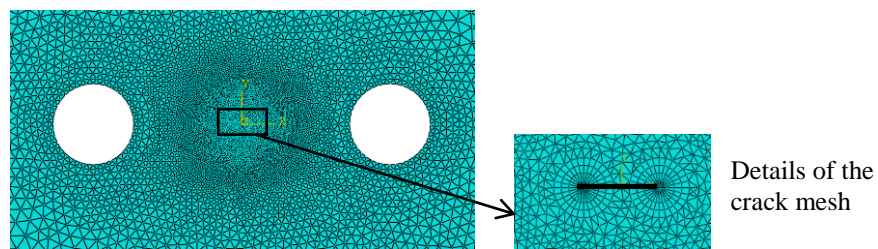


Fig. 2 Mesh with quadratic triangular elements

angle  $\gamma$  with respect to the axis  $X$ . A stress of 70 MPa, along to the  $Y$  axis, is applied to the first end of the composite material while the other end fixed.

The Simulation of linear tensile behavior and the influence of fiber orientation and other parameters, have been treated by the computer code Abaqus (Abaqus Standard Version 6.10.2010) and this for the analysis of composite structures by the finite element method. This code provides a complete system, incorporating not only the actual computing functions, but also the model construction functions (preprocessor) and outcomes treatment (post-processor). To properly conduct this study, we chose a shell element whose elements are triangular of quadratic type Fig. 2.

### 3. Theory and results

#### 3.1 Theory

The fracture mechanics (FM) has been essentially used for the study of macroscopic cracks: it applies when there are such discontinuities in the material that change the state of stress, strain and displacement. Knowledge of the different cracking regimes, the prediction of propagation speed and the control of cracking directions are essential for optimal design of mechanical parts, and, more simply, to avoid accidents. This study is limited to cases where the material behavior is linearly elastic; in the elastic domain of linear fracture mechanics (LFM) the value of the integral  $J$  represents the energy release rate for the propagation planar cracks, as shown by Rice (1968). The expression of the integral  $J$  is given by

$$J = \int_{\Gamma} \left( W dx_2 - t \cdot \frac{\partial u}{\partial x_1} ds \right) \quad (1)$$

Where:

$W(x_1, x_2)$  is the energy density of deformation,

$x_1, x_2$ : are the two directions,

$t = n \cdot \sigma$ : is the traction vector,

$n$ : is the normal to the curve  $\Gamma$ ,

$\sigma$ : is the Cauchy stress tensor,

$u$ : is the displacement vector.

The strain energy is given by

$$W = \int_0^{\epsilon} \sigma : d \epsilon; \quad \epsilon = \frac{1}{2} [\nabla u + (\nabla u)^T] \quad (2)$$

The  $J$ -integral around a crack front is frequently expressed in its general form (the Einstein notation) by

$$J_i = \lim_{\epsilon \rightarrow 0} \int_{\Gamma_{\epsilon}} \left( W n_i - n_j \sigma_{jk} \cdot \frac{\partial u_k}{\partial x_i} \right) d\Gamma \quad (3)$$

Where:

$J_i$  is the component of  $J$ -integral for a crack opening in  $x_i$  direction

$\epsilon$  is a small area near the crack front.

#### 3.2 Results

##### 3.2.1 Model without crack

Figs. 4(a) and 4(b) represent the distribution and the intensity of the Von Mises equivalent stress respectively for the embedding and the cancellation of imposed along the  $Y$  axis. We noticed that stress level of the first boundary condition (recessed) is more intense than that of the second condition ( $U_y=0$ ). The strongest constraints are localized at both notches level.

The graph in Fig. 5 is determined for a laminate without cracks. The results obtained numerically by the finite element method strongly depend on the boundary conditions imposed on

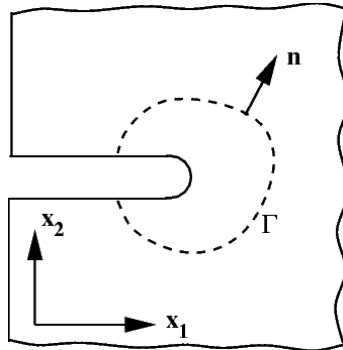
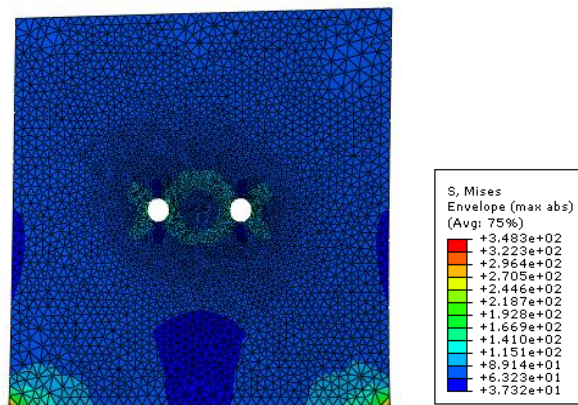
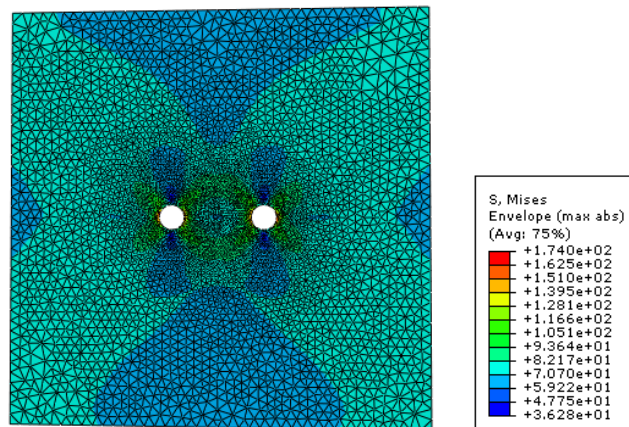


Fig. 3 Curve (outline) defined for J integral around a notch in two dimensions



(a) The case of recessed



(b) The case of displacement along the Y axis ( $U_y=0$ )

Fig. 4 Contour of the equivalent Von Mises stress for fiber orientation of  $30^\circ$

the boundary of the geometric model. For this reason we studied the intensity and stress distribution for the two following boundary conditions:

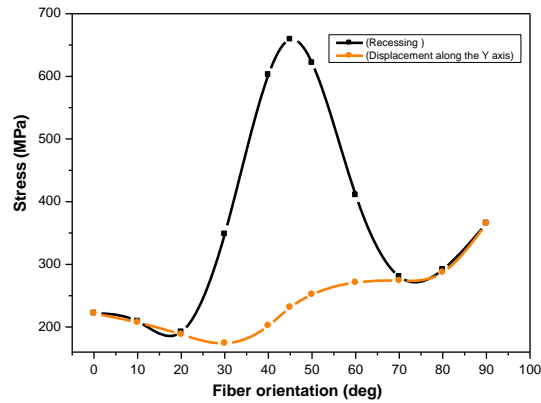


Fig. 5 Evolution of the equivalent Von Mises stress depending on fiber orientations for a composite plate without cracks for two boundary conditions: recessed and displacement along the Y axis ( $U_2=0$ )

Case 1: One end recessed

One of two ends of the composite material is embedded and the other is exposed to a uniformly distributed load over its surface, the applied stress is 70 MPa in the direction of the y axis.

Fig. 5 shows that the maximum Von Mises stresses are located at the recessed end and well above the applied stress. This curve has three peaks corresponding to the directions 40°, 45° and 50°, which are dangerous for the structure because they lead to maximum stresses. For these reasons we opted for a second mode of fixation.

Case 2: Elimination of displacement along the y axis

It is important to remember that the material is subjected to the same stress. Fig. 5 has the same shape that of the first curve but the peaks are completely reduced and that for the 30° orientation the composite material behaves better than a homogenous material, which is advantageous with respect to case 1.

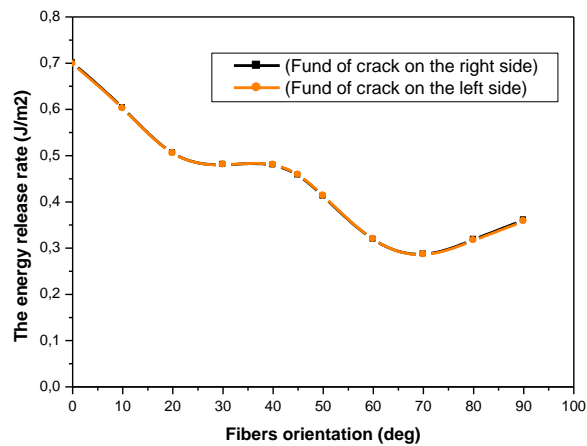


Fig. 6 Variation of energy release rate versus the fiber orientation for both crack.

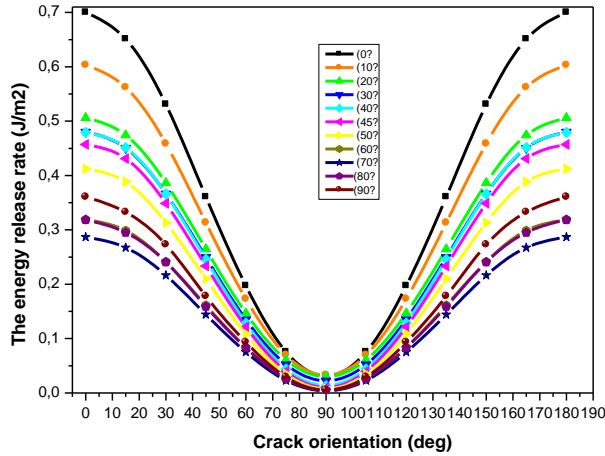


Fig. 8 Variation of the energy release rate in function of the orientation of the cracks for all orientations of the fibers where the two circular notches are horizontal

### 3.2.2 Model with the presence of a crack

The crack length of 1 mm is initiated in the middle of the laminate plaque, it is more precisely between the two circular notches placed horizontally ( $\gamma=0$ ) and is oriented at an angle  $\beta=0$  relative to the X axis. Fig. 6 illustrates the variation of energy release rate versus the fibers orientation angle  $\alpha$  for both bottoms of the crack; the results clearly show that the two curves are identical. For this reason, we numerically determined by the finite element method the rate of energy release for one of the two bottoms of the crack and the results subsequently obtained are determined only for the right bottom of the crack.

### 3.4 Effect of the fiber orientation on energy G

#### Case: $\gamma=0^\circ$ and variable angle $\alpha$

Fig. 7 shows the variation of the parameter G versus the angle  $\alpha$  and for all orientations of the crack when the notches are placed along the axis X. It is noted that the two curves, which respectively correspond to directions of angles crack  $\pi-\beta$  and  $\beta$ , are totally mixed together, which shows the parameter G symmetry relative to the axis Y. We note that whatever the angle of orientation of the fibers, the G factor proportionally decreases for the angle  $\beta$  from  $0^\circ$  to  $90^\circ$  and then rises again with augmentation of the angle  $\beta$  in the range  $[90^\circ, 180^\circ]$ . We observe that whatever the angle  $\beta$ , the factor G decreases with the rise of the angle of orientation of the fibers through three extreme points which correspond to the angles  $\alpha=30^\circ$ ,  $\alpha=40^\circ$  and  $\alpha=70^\circ$ . The energy release rate G is almost zero for the angle  $\beta=90^\circ$  and this is regardless of the fiber orientation.

### 3.5 Effect of the crack orientation on energy G

#### Case: $\gamma=0^\circ$ and variable angle $\beta$

The crack is rotated around the Z axis and its position is defined relative to an X axis by angle  $\beta$ . Fig. 8 shows the variation of the energy release rate versus the angle  $\beta$  for different orientations of the plies. From this figure, we notice that the shape of the curve is parabolic and the G factor

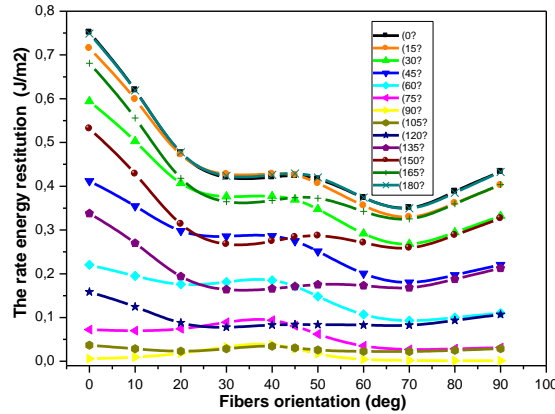


Fig. 9 Variation of the energy release rate in function of the fiber orientation for all orientations of the crack in the case where the two circular notches are inclined at an angle of 45°

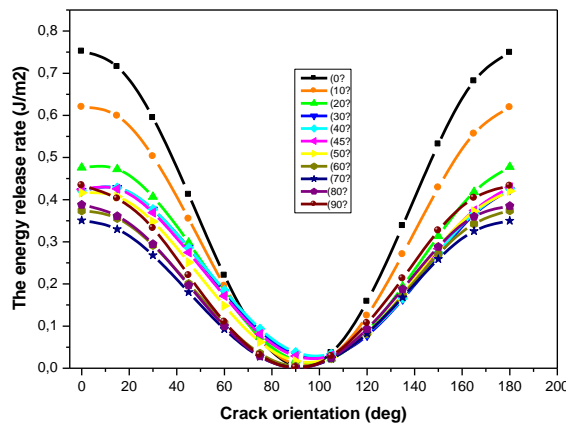


Fig. 10 Variation of the energy release rate in function of the cracks orientation for all orientations of the fibers where the two circular notches are inclined at an angle of 45°

reaches a minimum value for an angle  $\beta=90^\circ$  and this regardless of the angle  $\alpha$ . The higher  $G$  factor values are obtained for the crack oriented perpendicularly to the loading, which leads to its propagation in the material. The fiber orientation at an angle  $\alpha=70^\circ$ , at least, avoids more crack propagation compared to the other orientations of the plies.

### 3.6 Effect of the fibers orientation on energy $G$

#### Case: $\gamma=45^\circ$ and variable angle $\alpha$

Fig. 9 illustrates the variation of  $G$  factor as a function of the two angles  $\alpha$  and  $\beta$  and an orientation angle of the circular notches  $\gamma=45^\circ$ . It is noted that the curves are almost similar to that of Fig. 7 but the symmetry for factor  $G$  with respect to the  $Y$  axis is not maintained except for the angles of the fibers ranging from  $60^\circ$  to  $90^\circ$ . It is noted that the speed of propagation of the crack is greater when it is oriented at an angle  $\beta=0$  and this regardless of the fibers orientation. Note also

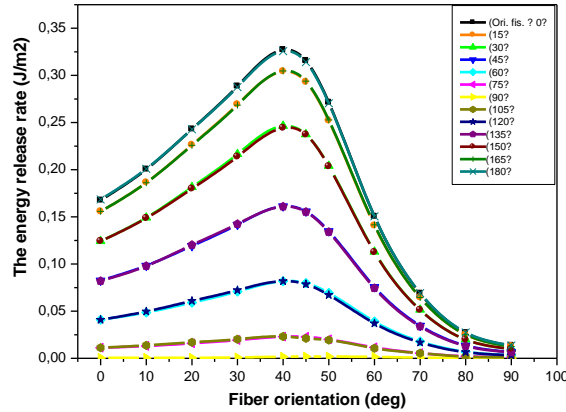


Fig. 11 Variation of the energy release rate in function of the fiber orientation for all orientations of the crack in the case where the two circular notches are vertical

that the orientation of the plies at an angle of 70° results in a low crack propagation.

### 3.7 Effect of the crack orientation on energy G

#### Case: $\gamma=45^\circ$ and variable angle $\beta$

Fig. 10 shows the variation of the energy release rate versus the angle  $\beta$  for different fiber orientations. From this figure, we notice that the shape of the curves is the same as those of Fig. 8, the  $G$  factor reaches a minimum value for an angle  $\beta=90^\circ$  and this, regardless of the angle  $\alpha$ . The numerical results determined by the finite element method are similar to those obtained in Fig. 5. The fibers orientation at an angle  $\alpha=70^\circ$  results in a low crack propagation compared to the other directions of the folds which confirms results obtained previously.

### 3.8 Effect of the fiber orientation on energy G

#### Case: $\gamma=90^\circ$ and variable angle $\alpha$

Fig. 11 illustrates the variation of the parameter  $G$  versus the angle  $\alpha$  and for all orientations of the crack when the notches are placed along the  $Y$  axis. It is observed that the two curves which respectively correspond to directions of angles crack  $\beta$  and  $\pi-\beta$  are identical, which shows a symmetry of the  $G$  parameter with respect to the  $Y$  axis and also notes that the energy release rate is almost equal to zero for the angle  $\beta=90^\circ$  and this regardless of the orientation of the fibers. The  $G$  parameter reaches a maximum value for plies orientation with  $\alpha=40^\circ$  and this is regardless of the orientation of the crack and then it tends to an asymptotic value relatively low when the fiber orientation is at an angle  $\alpha=90^\circ$  and therefore the crack does not spread if it is oriented along the  $Y$  axis regardless of the orientation of the fibers.

### 3.9 Effect of the crack orientation on energy G

#### Case: $\gamma=90^\circ$ and variable angle $\beta$

The variation of energy release rate versus  $\beta$  angle, for different folds orientations, is presented

in Fig. 12. This clearly shows that the curves have the same shape as that in Figs. 8 and 11 and the energy release rate  $G$  reaches a minimum value for an angle  $\beta=90^\circ$ , regardless of the angle  $\alpha$ . The highest values for  $G$  factor are obtained for folds oriented at an angle  $\alpha=40^\circ$ , which leads to a

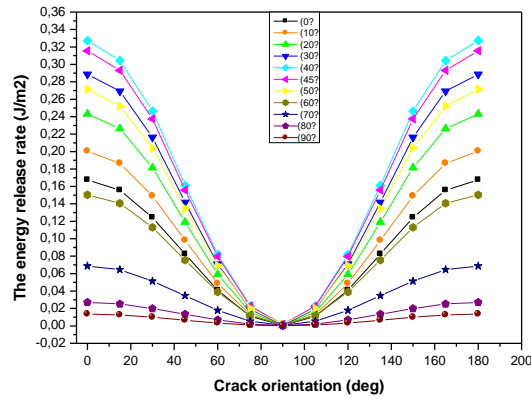


Fig. 12 Variation of the energy release rate in function of the cracks orientation for all orientations of the fibers where the two circular notches are vertical

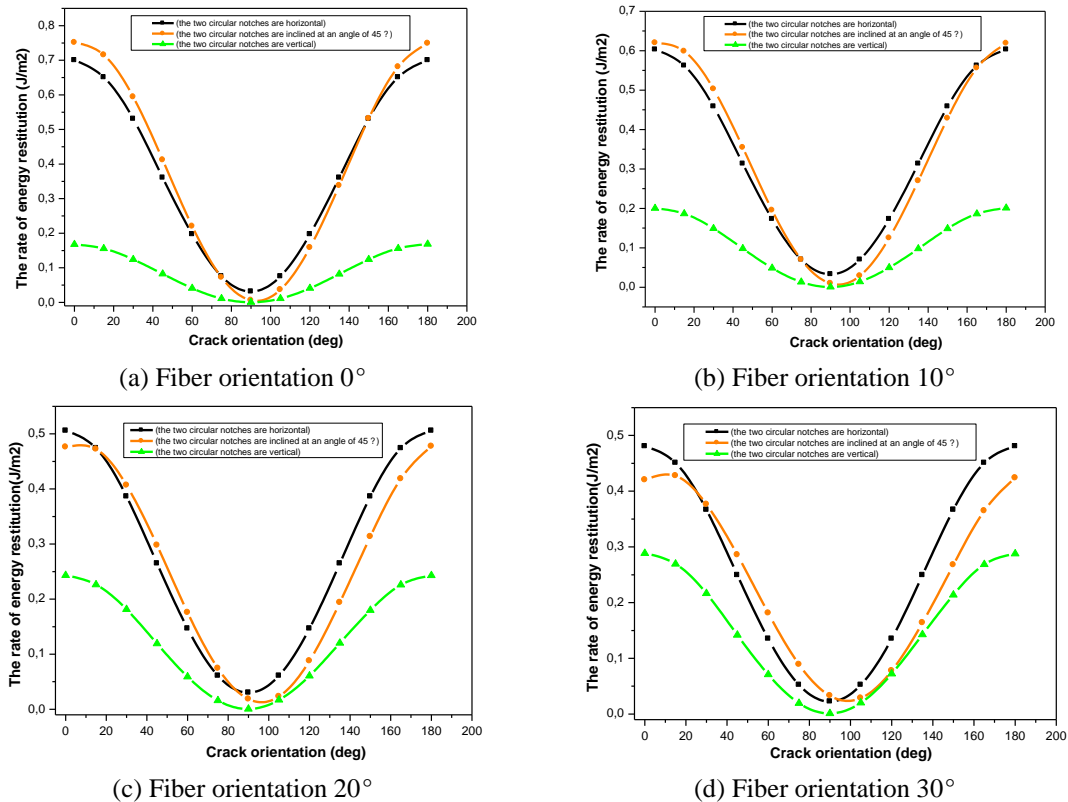
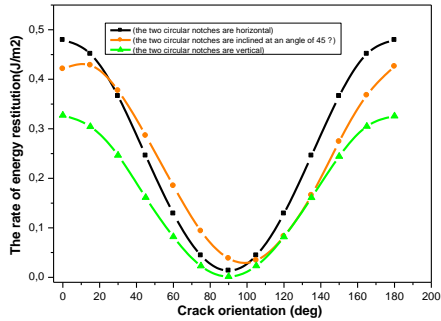
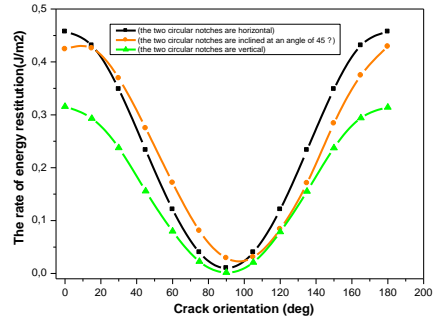


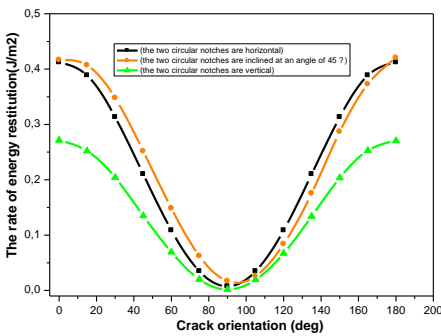
Fig. 13 Variation of the energy release rate in function of the crack orientation for three positions of the circular notches and different fiber orientations



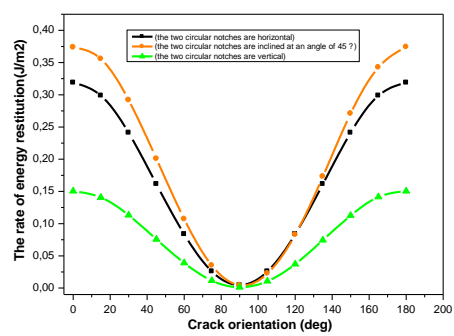
(e) Fiber orientation 40°



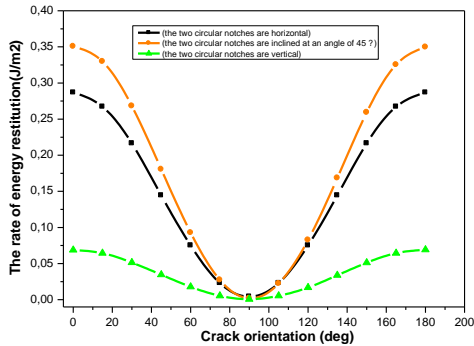
(f) Fiber orientation 45°



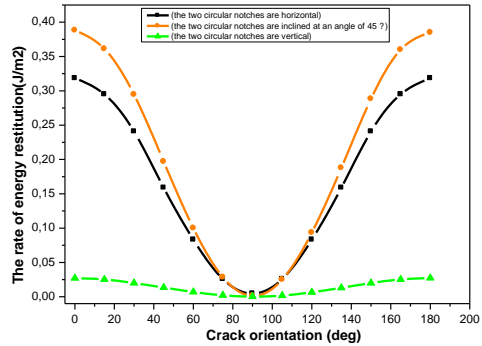
(g) Fiber orientation 50°



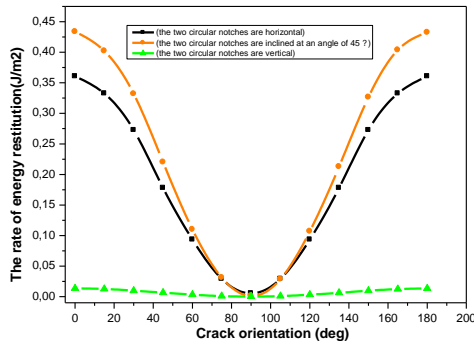
(h) Fiber orientation 60°



(i) Fiber orientation 70°



(j) Fiber orientation 80°



(k) Fiber orientation 90°

Fig. 13 Continued

faster propagation of the crack than other fiber orientations. The results determined numerically by the finite element method confirm those obtained previously in Fig. 11.

### 3.10 Effect of orientation of the two circular notches angle $\gamma$ on energy $G$

The variations of the energy release rate  $G$  versus the  $\beta$  angle and for three positions of circular notches ( $\gamma=0^\circ$ ,  $\gamma=45^\circ$  and  $\gamma=90^\circ$ ) are shown in Fig. 13. Each graph is determined for a ply orientation from  $0^\circ$  to  $180^\circ$ . We note that the two curves corresponding to the two positions of the holes ( $\gamma=0^\circ$  and  $\gamma=45^\circ$ ) are almost identical for different orientations of folds, regardless of the crack angle  $\beta$ . However, we observe a significant change in the parameter  $G$  for the notches placed vertically along the  $Y$  axis. The factor  $G$  gradually increases for fiber orientation in the range  $[0^\circ-40^\circ]$  and then decreases to zero in the range  $[40^\circ-90^\circ]$ , and this for different crack angles  $\beta$ . We also note that the release rate is zero for a crack oriented along the loading direction, preventing its spread to the three positions of the circular notches and for all folds orientations.

### 3.11 Effect of mechanical properties.

Fig. 14 shows the variation of the energy restitution rate  $G$  for both laminated composite materials as follows:

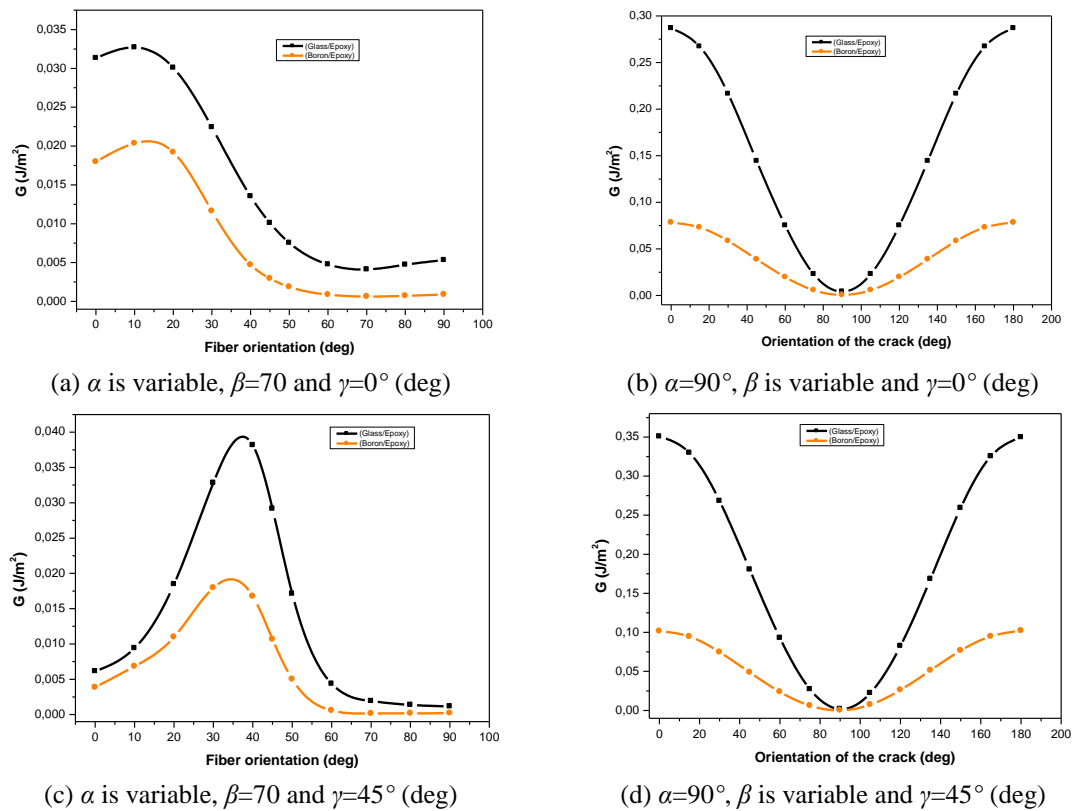


Fig. 14 Variation of the energy restitution rate versus fibers orientation for two materials

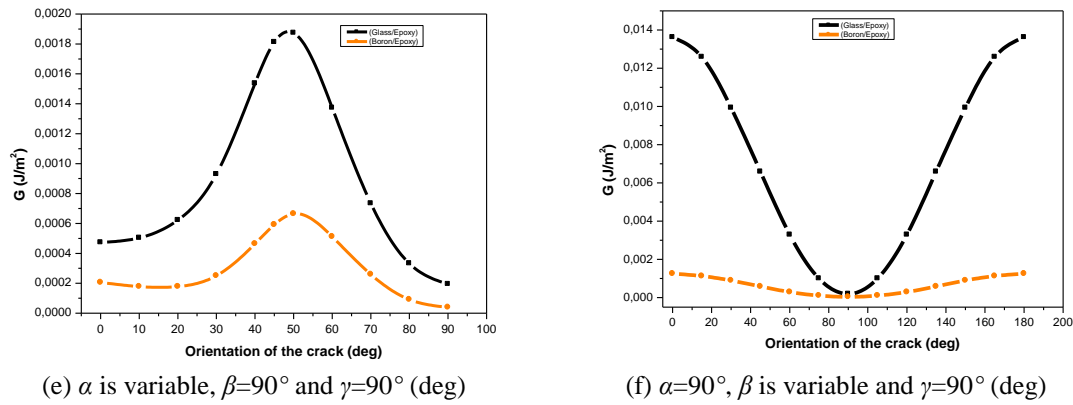


Fig. 14 Continued

-Figs. (a), (c) and (e): versus fibers orientation  $\alpha$ , with constant  $\beta$  for notches placed at  $0^\circ$ ,  $45^\circ$  and  $90^\circ$ .

-Figs. (b), (d) and (f) versus crack orientation  $\beta$ , with  $\alpha$  constant for notches placed at  $0^\circ$ ,  $45^\circ$  and  $90^\circ$ .

This figure shows that whatever the orientation of the fibers, of the crack or of the two notches, the composite material boron/epoxy behaves better than the composite material glass/epoxy regarding the crack propagation and this because of its mechanical properties.

#### 4. Conclusions

The aim of this numerical study was to analyze the energy release rate under the influence of mechanical properties and parameters such as fiber orientation, crack orientation and orientation of the two circular notches.

This study allowed us to draw the following conclusions:

- The fiber orientation has a significant effect on the crack propagation. The fibers oriented between  $70^\circ$  and  $90^\circ$  reinforce better the composite structure and mitigate the crack propagation regardless of its orientation.

- The variation of the energy release rate  $G$  of composite glass/epoxy versus the angle  $\beta$  and for circular notches position  $\gamma=90^\circ$ , reaches zero regardless of the crack angle  $\beta$ . We also note that the energy release rate is zero for a crack oriented along the loading direction, preventing its spread for the three positions of circular notches and for all fibers orientations.

- Whatever the orientation of the fibers, of the crack or of the two notches, the composite material boron/epoxy behaves better than the composite material glass/epoxy material regarding of the crack propagation and this because of its mechanical properties.

- The material type has practically no effect on the parameter  $G$  when the crack is parallel to the loading.

As perspectives to this analysis, we will consider two research panes:

- The study of the stresses concentration intensity factor of crossed laminates composite subjected to the same loadings.

- The life span of the laminate composite under effect of cyclic loads.

## References

- Achache, H., Boutabout, B. and Ouinas, D. (2013), "Mechanical behavior of laminated composites with circular holes", *Key Eng. Mater.*, **550**, 1-8.
- Bai, T. and Pollard, D.D. (1999), "Spacing of fractures in a multilayered fracture saturation", *Int. J. Fract.*, **100**(4), 23-24.
- Berthelot, J.M. and Le Corre, J.F. (2000), "Statistical analysis of the progression of transverse cracking and delamination in cross-ply laminates", *Compos. Sci. Tech.*, **60**(3), 2659-2669.
- Bouziane, S., Bouzard, H., Boulares, N. and Guenfoud, M. (2014) "Energy release rate for kinking crack using mixed finite element", *Struct. Eng. Mech.*, **50**(5), 665-677.
- Das, S., Choudhury, P., Halder, S. and Sriram, P. (2013), "Stress and free edge delamination analyses of delaminated composite structure using ANSYS", *Procedia Eng.*, **64**, 1364-1373.
- Haneef, M., Shabbir Ahmed, R.M. and Ali, M.M. (2011), "Studies on delaminating effects on stress development in composite structures", *Proceedings of the World Congress on Engineering*, Vol. III WCE, July, London, U.K.
- Katerelos, D.T.G., Kashtalyan, M., Soutis, C. and Galiotis, C. (2008), "Matrix cracking in polymeric composites laminates Modeling and experiments", *Compos. Sci. Tech.*, **68**(12), 2310-2317.
- Manders, P.W., Chou, T.W., Jones, F.R. and Rock, J.W. (1983), "Statistical analysis of multiple fracture in 0/90/0 glass fiber/epoxy laminates", *J. Mater. Sci.*, **18**, 2876-2889.
- Product Dassault Systèmes Simulia Corp (2010), ABAQUS Standard Version 6.10, Providence, RI, USA.
- Qing, G.H., Liu, Y.H. and Li, D.H. (2011), "A semi-analytical model for the energy release rate analyses of composite laminates with a delamination", *Finite Elem. Anal. Des.*, **47**, 1017-1024.
- Rebière, J.L., Maâtallah, M.N and Gamby, D. (2002), "Analysis of damage mode transition in a cross-ply laminate under uniaxial loading", *Compos. Struct.*, **55**, 115-126.
- Rice, J.R. (1968), "A path independent integral and the approximate analysis of strain concentration by notches and cracks", *J. Appl. Mech.*, **35**(2), 379-386.
- Seo, D.C. and Lee, J.J. (2002), "Fatigue crack growth behavior of cracked aluminum platerepaired with composite patch", *Korea, Compos. Struct.*, **57**, 323-330.
- Smith, B.W. (1993), *Fractography for Continuous Fiber Composites*, Dans, Engineered Materials Handbook, Volume 1: Composite, Ohio, USA, ASM International.
- Szekrényes, A. (2012), "Interlaminar stresses and energy release rates in delaminated orthotropic composite plates", *Int. J. Solid. Struct.*, **49**, 2460-2470.
- Todo, M. and Jar, P.Y. (1998), "Study of mode-I interlaminar crack growth in DCB specimens of fibre-reinforced composites", *Compos. Sci. Tech.*, **58**, 105-118.
- Todo, M., Jar, P.Y. and Takahashi, K. (2000), "Initiation of a mode-II interlaminar crack from an insert film in end-notched flexure composite specimen", *Compos. Sci. Tech.*, **60**, 263-272.
- Wang, J. and Karihaloo, B.L. (1997), "Matrix crack-induced delamination in composite laminates under transverse loading", *Compos. Struct.*, **38**, 661-666.
- Yao, L.J., Alderliesten, R.C., Zhao, M.Y. and Benedictus, R. (2014), "Discussion on the use of the strain energy release rate for fatigue delamination characterization", *Compos. Part A*, **66**, 65-72.